



Geometric coercivity scaling in magnetic thin film antidot arrays

I. Ruiz-Feal^a, L. Lopez-Diaz^a, A. Hirohata^a, J. Rothman^a, C.M. Guertler^a,
J.A.C. Bland^{a,*}, L.M. Garcia^b, J.M. Torres^b, J. Bartolome^b, F. Bartolome^b,
M. Natali^c, D. Decanini^c, Y. Chen^c

^a*Cavendish Laboratory, University of Cambridge, Madingley Road, Cambridge CB3 0HE, UK*

^b*Instituto de Ciencia de Materiales de Aragon, CSIC-Universidad de Zaragoza. 50009 Zaragoza, Spain*

^c*L2M Laboratories-CNRS, 196 Avenue Henry Ravera, 92225 Bagneux Cedex, France*

Abstract

We have investigated the magnetic properties of periodic arrays of circular antidots fabricated from epitaxial Fe/GaAs(001) thin films using magnetic force microscopy, micromagnetic simulations, and AGFM and SQUID magnetometry. A linear dependence between the coercivity of the film and geometrical array parameters has been found suggesting a way to engineer the coercive field in ferromagnetic thin films. © 2002 Published by Elsevier Science B.V.

Keywords: Nanoparticles; Coercivity; Domain pattern

During the last few years there has been much interest in artificially engineering, the magnetic properties of thin films using novel micron and sub-micron lithographic techniques. Previous theoretical and experimental studies [1–4] suggest that the magnetic properties of magnetic films can be controlled by artificially produced arrays of holes (antidots). In this work, we discuss the magnetic properties of epitaxial Fe/GaAs(001) films structured into periodic 2-D circular antidot arrays of varying size and separations.

A 30 nm epitaxial Fe(001) film was grown on GaAs(001) using molecular beam epitaxy (MBE) techniques [5]. Four antidot arrays (diameter $D = 1$ and $2 \mu\text{m}$, and periodicity $\lambda = 1.1D$ and $2D$) were then patterned into this film using X-ray lithography techniques [6]. The array axes were oriented at 45° with respect to the crystallographic easy axes, i.e. the crystallographic [100] of the Fe corresponds to the [011] direction of the array.

The magnetic moment of the sample parallel to the applied magnetic field was measured with an alternating gradient field magnetometer (AGFM) [8] and a commercial SQUID MPMS5 QUANTUM DESIGN. The Fe antidot structures were observed in the remanent state by magnetic force microscopy (MFM) together with atomic force microscopy (AFM) with resolution of 100 and 10 nm, respectively [7]. Micromagnetic simulations were carried out in order to investigate the magnetisation configurations induced by the antidots. The computational region, of dimensions $\lambda \times \lambda \times t$, corresponds to one period (λ) and thickness (t) of the array and periodic boundary conditions were imposed. This computational region was discretised in a two-dimensional square mesh and the equilibrium equation was solved numerically in order to find the equilibrium configuration for a given applied field. A conjugate gradient solver was used. Typical parameters of bulk Fe at room temperature have been used.

Fig. 1 shows MFM images of the remanent states after saturation along the easy (a) and hard (c) magnetocrystalline axes, respectively. These images are compared with the remanent states computed by micromagnetic simulations after saturation along the

*Corresponding author: Tel.: +44-1223-337436; fax: +44-1223-350266.

E-mail address: jacob1@phy.cam.ac.uk (J.A.C. Bland).

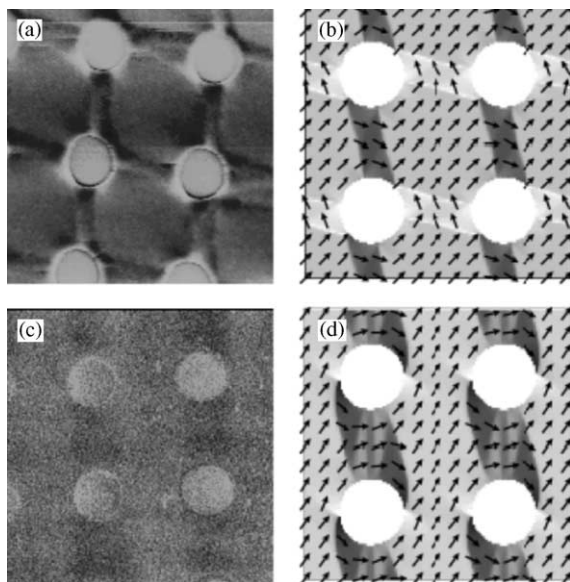


Fig. 1. MFM (a,c) and micromagnetic simulations (b,d) images of the remanent state after saturation along magneto-crystallographic easy (a,b) and hard (c,d) axes.

easy (b) and hard (d) axes as well. An excellent agreement between both images can be seen. Similar domain configurations to the one in Fig. 1(a) have been found for antidot systems in permalloy films [3] in which no relevant magnetic anisotropies were present. The ones shown in this work show a more clear domain configuration because the magnetic anisotropies sharpen the domain walls.

Fig. 2 shows AGFM hysteresis loops of all arrays. A double switch reversal mechanism is seen in all cases. In the easy axis measurements, a first jump occurs at approximately the coercive field of the un-patterned Fe film. The samples remain at approximately the same magnetisation value when the field is increased until a second jump occurs and the sample is saturated. Equivalent features are seen in the hard axis but with an additional rotation at high fields. The magnetic field of the first jump is approximately the same in all samples, whereas the field at which the second jump is launched depends on the sample. The magnetisation value of the intermediate stable state in the samples with $\lambda = D$ is approximately the same ($0.72M_s$), and the same happens for samples with $\lambda = 0.1D$ but with a different value ($0.86M_s$). SQUID measurements also performed show the same results.

The samples consisted of a $2 \times 2 \text{ mm}^2$ Fe film, in which an area of $0.8 \times 0.8 \text{ mm}^2$ was patterned with antidots. This means that 16% of the area of the sample was a patterned region, and 84% un-patterned. In the patterned region, 19.6% of the Fe was removed for

samples with $\lambda = 2D$, and that number was 64.9% for samples with $\lambda = 1.1D$. Thus, for samples with $\lambda = 2D$, 13% of the magnetic moment comes from the patterned region, whereas this number is 6.3% for samples with $\lambda = 1.1D$. Using samples with $\lambda = 2D$ as an example, if only the un-patterned region had reversed, the measured magnetisation would be $(1 - 2 \times 0.13)M_s = 0.74M_s$. For samples with $\lambda = 1.1D$ this number is $0.87M_s$. Both numbers reasonably agree with measurements. These values correspond with the magnetisation that would be measured if only the un-patterned film that surrounds the antidots had reversed. Therefore, we can conclude that the first jump in the hysteresis loop is due to the reversal of the un-patterned film that surrounds the area with the antidots, and the second one is due to the central area of the samples, highly influenced by the antidot array.

The contribution of the patterned area to the hysteresis loops was studied by subtracting from easy axis AGFM hysteresis loops a loop obtained from an un-patterned sample. After these subtractions it was seen that the coercive field (H_c^*) of the patterned area increases as the antidot size and the periodicity of the array decrease. We have investigated phenomenological laws that describe the geometry of the array by one single parameter. We have found that the coercive field is approximately linearly dependent on $1/(\lambda - D)$. This result is shown in Fig. 3. A fundamental explanation for this phenomenological law is beyond the scope of this work. Nevertheless, $\lambda - D$ is the separation between closest antidots. Both the dipolar field and the pinning effects of the antidots are expected to be stronger the closer the antidots are. Therefore, the higher $1/(\lambda - D)$ is, the higher the external field necessary to overcome the dipolar fields and the domain wall pinning effects along the antidot sample. Equivalent phenomenological laws, in which coercivity is proportional to t/x , where t represents the thickness of the film and x a length parameter of the magnetic nanostructure, have been found for both dots [9] and wires [10].

In conclusion, we have studied the magnetic properties of antidot arrays patterned on epitaxial Fe/GaAs(001) thin films. The presence of the antidots leads to the formation of well-defined domain configurations that would determine the magnetisation reversal of the system. A phenomenological linear relationship between the coercive field of the antidots and the geometrical array parameters ($1/(\lambda - D)$) has been found. This opens the possibility of creating ferromagnetic films with a desired coercive field; i.e. engineering the coercive field of a ferromagnetic film.

The authors would like to thank the European Commission for financial support under the Marie Curie Scheme, 4th framework program, contract num-

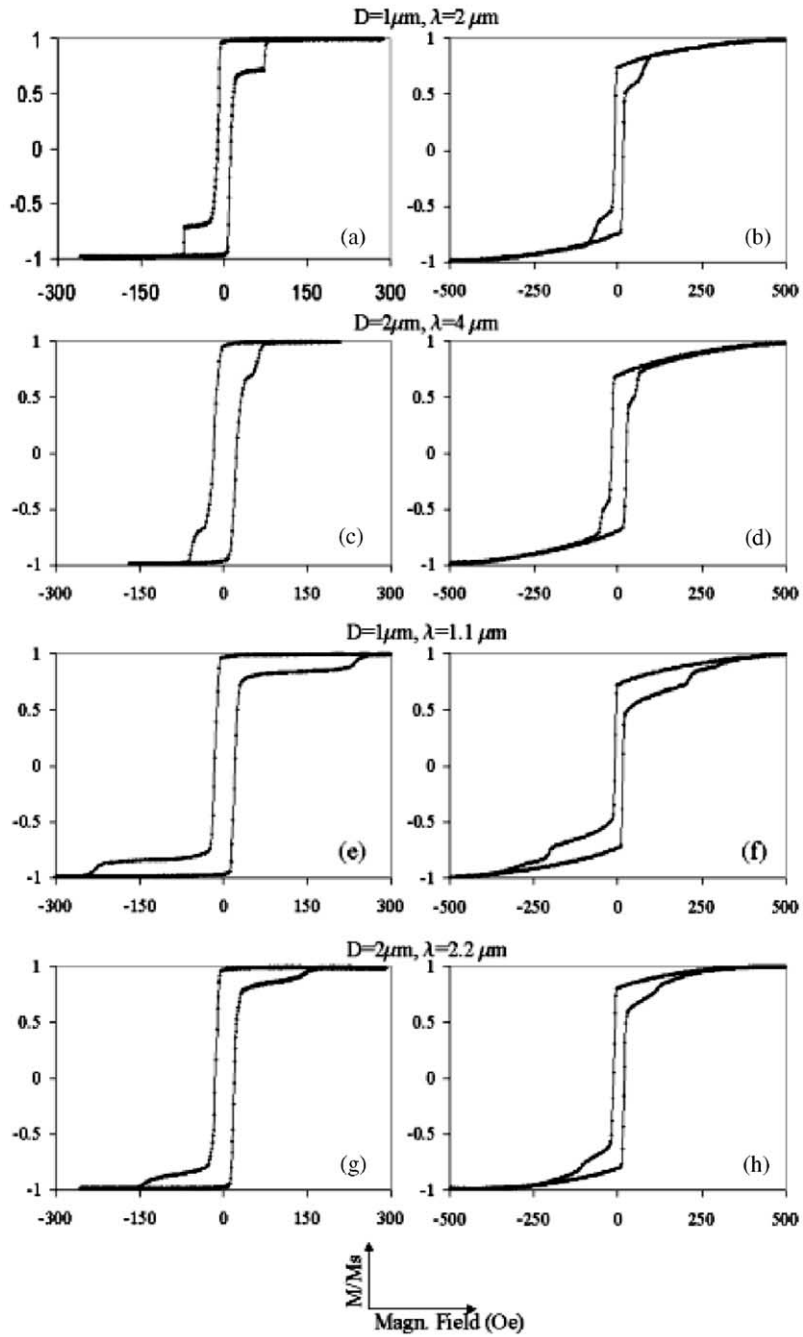


Fig. 2. AGFM measurements of all the samples, both along easy (a,c,e,g) and hard (b,d,f,h) axes.

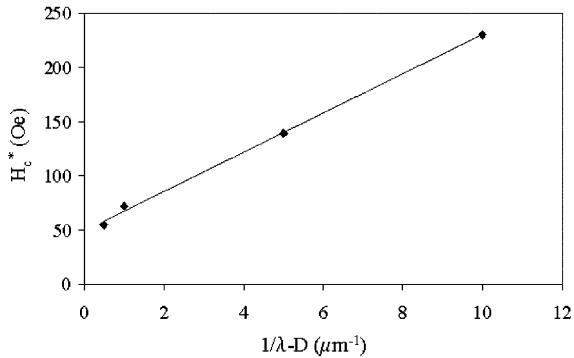


Fig. 3. Dependence of coercive field of antidots on $1/(\lambda - D)$.

ber ERBFMBICT983157, 5th framework program, contract number HPMF-1999-00141, and under the MASSDOTS project (ESPRIT LTR programme, Project number 22464). The Spanish team acknowledges financial aid from CICYT project MAT99/1142.

References

- [1] L. Torres, L. Lopez-Diaz, J. Iñiguez, Appl. Phys. Lett. 73 (25) (1998) 3766.
- [2] A.O. Adeyeye, J.A.C. Bland, C. Daboo, Appl. Phys. Lett. 70 (23) (1997) 3164.
- [3] C.T. Yu, H. Jiang, L. Shen, P.J. Flanders, G.J. Mankey, J. Appl. Phys. 87 (9) (2000) 6322.
- [4] I. Guedes, N.J. Zaluzec, M. Grimsdich, V. Metlushko, P. Vavassori, B. Ilic, P. Neuzil, R. Kumar, Phys. Rev. B 62 (17) (2000) 11 719.
- [5] C.M. Guertler, Y.B. Xu, J.A.C. Bland, J. Magn. Magn. Mater. 226–230 (2001) 655.
- [6] O. Fruchart, J.P. Nozieres, B. Keevorkian, J. Toussaint, D. Givord, F. Rousseaux, D. Decanini, F. Carcenac, Phys. Rev. B 57 (1998) 2596.
- [7] K.L. Babcock, M. Dugas, Appl. Phys. Lett. 69 (1996) 705.
- [8] P.J. Flanders, J. Appl. Phys. 63 (8) (1998) 3940.
- [9] O. Fruchart, J.-P. Nozieres, W. Wernsdorfer, D. Givord, Phys. Rev. Lett. 82 (6) (1999) 1305.
- [10] A.O. Adeyeye, J.A.C. Bland, C. Daboo, J. Magn. Magn. Mater. 188 (1998) L1.